



Hot cracking in cast alloy 718

Downloaded from: <https://research.chalmers.se>, 2026-05-15 07:46 UTC

Citation for the original published paper (version of record):

Singh, S., Andersson, J. (2018). Hot cracking in cast alloy 718. *Science and Technology of Welding and Joining*, 23(7): 568-574. <http://dx.doi.org/10.1080/13621718.2018.1429238>

N.B. When citing this work, cite the original published paper.

Hot cracking in cast alloy 718

Sukhdeep Singh ^a and Joel Andersson ^b

^aDepartment of Industrial and Materials Science, Chalmers University of Technology, Gothenburg, Sweden; ^bDepartment of Engineering Science, University West, Trollhättan, Sweden

ABSTRACT

Hot cracking susceptibility of the Fe–Ni-based precipitation hardening cast superalloy Alloy 718 was studied by Vareststraint weldability testing. The effect of two hot isostatic pressing (HIP) treatments commonly employed in the aerospace industry was investigated in reference to the as cast condition. It was found that the heat affected zone (HAZ) liquation cracking susceptibility increased for samples with pre-weld HIP treatments. The as cast condition disclosed the best response for liquation cracking followed by HIP-1120 (1120°C/4h (HIP) + 1050°C/1h and furnace cooling to 650°C/1h in vacuum + 950°C/1h) and HIP-1190 (1190°C/4h (HIP) + 870°C/10h and furnace cooling to 650°C/1h in vacuum + 950°C/1h). The amount of the secondary precipitates and base metal grain size was found to be important parameters influencing the cracking susceptibility. Regarding solidification cracking susceptibility, the three conditions appear to behave similarly.

ARTICLE HISTORY

Received 10 November 2017
Accepted 14 January 2018

KEYWORDS

Hot cracking; alloy 718; hot isostatic pressing; solidification cracking; liquation cracking; Vareststraint testing



Introduction

Alloy 718 is an Fe–Ni-based superalloy commonly used in high temperature exposed components in the rear end of aero engines. The alloy was first developed in the wrought form by Eiselstein in 1962 [1], with the main driving force to develop a superalloy being resistant to strain age cracking. Later on, the cast material was made available due to the significant progress of melting techniques (especially vacuum technology) and development of hot isostatic pressing (HIP) technology [2,3]. Nowadays, cast structural components are joined together with wrought components to tailor components in more efficient way and to reduce the costs in comparison to single piece castings. This manufacturing procedure, however, results in challenges in the welding process as the microstructure of cast materials is more complex than the wrought one due to the presence of high amount of segregation [4,5].

Nb is a key element in Alloy 718 when it comes to, e.g. segregation [6]. Its addition in the range of 5 wt-% is responsible for the formation of the main strengthening phase, gamma double-prime (γ''). The slower precipitation kinetics of γ'' in comparison to gamma prime (γ') phase makes it almost immune to strain age cracking. However, Nb is also responsible of forming other precipitates such as the primary metal carbide NbC, Laves and delta (δ) phase [5,7]. Its high tendency for segregation aid formation of NbC and Laves in the interdendritic regions of cast materials and

also weldments which is a contributing factor for hot cracking to occur.

Homogenisation of the material is assumed to be required after casting and prior to welding in order to reduce susceptibility towards hot cracking. The temperature and dwell time of the heat treatment influence the degree of homogenisation being required for dissolving critical phase constituents in the microstructure. In the aerospace industry it is common that structural components undergo HIP treatments. Through HIP, the objective is to improve the mechanical properties of the cast structure by closing any existing porosity at high pressure and high temperature in a controlled atmosphere. Two different approaches are commonly used in the industry when it comes to HIP of cast Alloy 718: one approach consists of HIP at 1120°C [8], the other one is performed at 1190°C [9,10], which are temperatures respectively below and above the incipient melting temperature of the Laves phase [9]. Extensive studies have covered predictive methodologies for crack growth in repaired and non-repaired engine stationary components [8,11] and repair weldability studies of cast Alloy 718 [8]. However, no comparative study exists to the authors' best knowledge regarding the influence of the two HIP treatments on hot cracking susceptibility. This leads to the motivation for the current study, which is to investigate the hot cracking susceptibility of cast Alloy 718 by Vareststraint (Variable Restraint) testing in the as cast condition and to compare it with cast Alloy 718

CONTACT Sukhdeep Singh  sukhdeep.singh@chalmers.se  Department of Industrial and Materials Science, Chalmers University of Technology, Gothenburg SE-412 96, Sweden

© 2018 The Author(s). Published by Informa UK Limited, trading as Taylor & Francis Group.

This is an Open Access article distributed under the terms of the Creative Commons Attribution-NonCommercial-NoDerivatives License (<http://creativecommons.org/licenses/by-nc-nd/4.0/>), which permits non-commercial re-use, distribution, and reproduction in any medium, provided the original work is properly cited, and is not altered, transformed, or built upon in any way.

being exposed to HIP treatments at 1120°C and 1190°C, respectively.

Experimental

The alloy composition is presented in Table 1. The complete details of the HIP conditions are represented in Table 2.

For each condition, 10 cast plates were received from the supplier with approximate dimensions of 300 × 60 × 12 mm. Each plate was electric discharge machined into six small test samples with approximate dimensions of 150 × 60 × 3.3 mm. A state-of-art Vareststraint weldability testing machine was used at test radii varying from 20 to 200 mm, corresponding to strain levels of 0.8%, 1.1%, 1.6%, 2.1%, 2.7%, 3.3%, 3.9% and 8.2%. The test set up is described elsewhere [12]. The strain (ϵ) is given by the following equation:

$$\epsilon = \frac{t}{2R} \quad (1)$$

where t is the thickness of the plate (3.3 mm) and R is the die radius. For each die radii and condition a total of seven plates were tested. The welding and testing parameters are based from a DOE study which produced the lowest average total crack length and lowest standard deviation among different settings [12]. The gas tungsten arc welding (GTAW) parameters are presented in Table 3.

The surfaces of the Vareststraint tested samples were manually polished by using abrasive paper Carbimet™ to remove any oxide layer and crack measurements were conducted by using stereo microscope at 57× magnification. Samples were cut and mounted using standard procedures and subsequently etched by Kalling's 2 (2g CuCl₂, 49 mL HCl, 40–80 mL ethanol) and etchant 13 (10 g oxalic acid, 100 mL water). Weld bead dimensions were measured on cross-sections obtained from the area experiencing maximum amount of bending, at a distance of 15 mm from the end of the weld. Microstructural evaluation was conducted by optical microscopy and scanning electron microscopy (LEO 1550 FEG-SEM with Oxford Electron Dispersive X-ray Spectroscopy).

Table 1. Composition of Alloy 718 in wt-%.

Ni	Fe	Cr	Nb	Mo	Ti	Al	Mn	Co	Cu	Si	C	S	P	B	V	W
52.98	Bal.	18.11	5.31	2.98	0.99	0.42	0.03	0.07	0.01	0.07	0.05	0.002	0.0009	0.003	< 0.1	< 0.01

Table 2. HIP treatments steps for cast Alloy 718.

Condition	HIP at 100 MPa	Post-HIP in vacuum	Solution heat treatment
HIP-1120 [8]	1120°C/4h	1050°C/1h + FC to 650°C in 1h	950°C/1h + AC
HIP-1190 [9,10]	1190°C/4h	870/10h + FC to 650°C in 1h	950°C/1h + AC

FC, furnace cooling; AC, air cooling.

Table 3. Welding parameters for GTAW during longitudinal Vareststraint testing [12]. Argon gas purity of 99.99%.

Welding speed (mm s ⁻¹)	Stroke rate (mm s ⁻¹)	Arc length (mm)	Welding current (A)	Ar gas flow (l min ⁻¹)
1	10	2	70	15

Results

Welds

Figure 1 shows the weld grain structures of the three conditions. The three sections are taken from plates tested at 2.7% augmented strain. It can be seen different weld grains structures occurred, with few and small equiaxed grains in the as cast condition and columnar grains in the HIP conditions.

Weld bead dimensions from plates tested at 4% augmented strain are disclosed in Table 4. Weld cross-sections can be seen in Figure 2.

It can be seen that the while width values were within tolerances, the penetration depths had major variations and overall weld shapes were different taking into consideration the undercut values.

Microstructure

As to be expected, the as cast condition showed high amount of segregation, with 3.7 volume fraction (Vv) of secondary precipitates (Table 5), in the interdendritic regions from Nb rich constituents (Laves and NbC). A detailed high-resolution image of the Laves eutectic can be seen in Figure 3.

In the HIP-treated conditions, the amount of segregation is much lower in comparison to as cast condition but with slight difference between HIP-1120 and HIP-1190. The evolution of the secondary phase precipitates in HIP treatments can be seen in Figure 4. Adjacent to them small amounts of delta phase precipitation was seen to occur.

Grain size measurements from Table 5 reveal the typical large grain size of cast materials. As cast has the lowest average grain size of 1.7 mm, followed by HIP-1120 (2.6 mm) and HIP-1190 (3.3 mm), respectively. No significant difference in base metal hardness was observed.

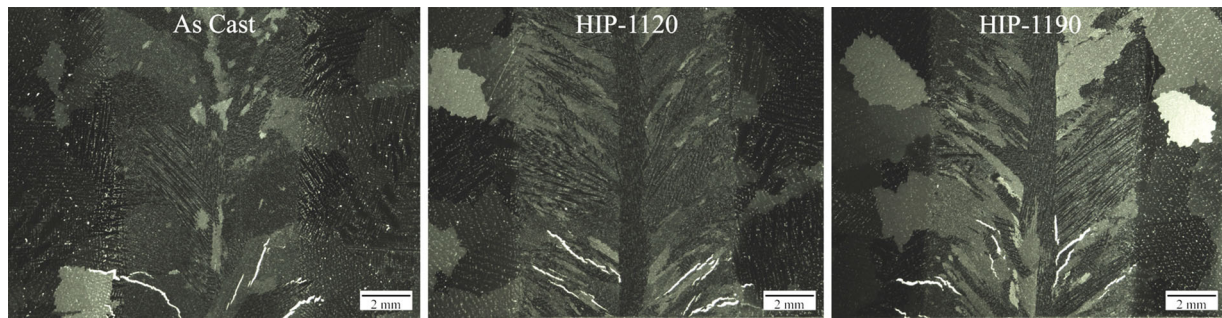


Figure 1. Weld grain structure and cracking in plates tested at 2.7% augmented strain.

Table 4. Weld bead dimensions taken by averaging measurements of three plates from each condition.

Condition	Depth (mm)	Width (mm)	Undercut (mm)	D/W
As Cast	4.03 ± 0.06	7.03 ± 0.12	0.4 ± 0	0.57 ± 0.02
HIP-1120	4.5 ± 0.17	7.43 ± 0.21	0.67 ± 0.25	0.61 ± 0.01
HIP-1190	3.93 ± 0.40	7.43 ± 0.21	0.31 ± 0.44	0.53 ± 0.05

Table 5. Volume fraction of secondary precipitates, grain size measurements and base metal hardness.

Condition	Vv (%)	GS (mm)	HV
As Cast	3.7 ± 0.6	1.7 ± 0.1	260 ± 20
HIP-1120	1.7 ± 0.1	2.6 ± 0.3	220 ± 30
HIP-1190	1.3 ± 0	3.3 ± 0.3	210 ± 20

Heat affected zone liquation cracking in the as cast condition was associated with liquation of the Laves eutectic, as can be visualised in Figure 5. On the other hand, in the HIP conditions, no large liquated Laves clusters were seen. The cracking followed along grain boundaries and was characterised by presence of eutectic constituents.

Varestraint testing

The average total crack length (Avg. TCL) values against augmented strain for fusion zone (FZ) graph is plotted in Figure 6. Cracking related to the HAZ liquation is shown in Figure 7.

Out of the original 168 test plates, 10 were excluded as the test did not proceed correctly. Rejection criteria were the S-shaped welds indicating the robot did not weld in straight line, and the tungsten electron tip hit the plate. Therefore, a few data points are missing in the plot. These points belong to three samples each for the as cast and HIP-1190 condition at 2.7% augmented strain and two samples each for the as cast and HIP-1120 at 3.2% augmented strain.

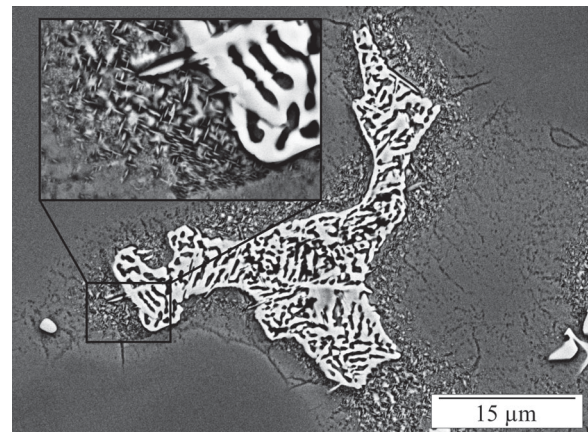


Figure 3. Backscattered SEM image of Laves phase with eutectic morphology surrounded small precipitates that resemble γ'' [6].

Discussion

Solidification cracking

The different grain structures in the weld metals suggest that thermal gradients were also different despite the welding conditions being the same. The example in Figure 1 from the as cast test plate, which showed more tortuous centreline with few equiaxed grains structure,

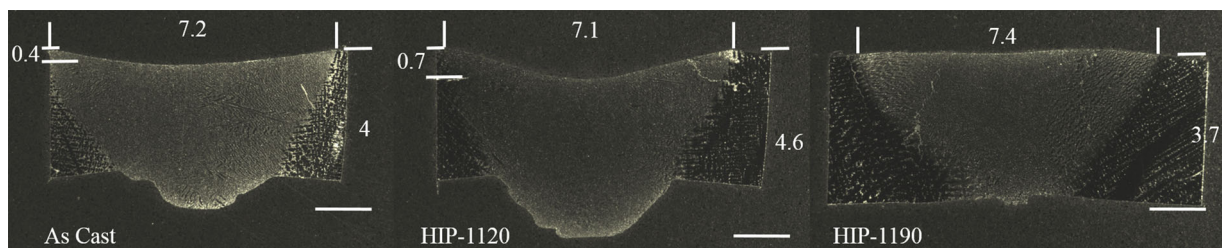


Figure 2. Weld cross-sections from plates tested at 4% augmented strain.

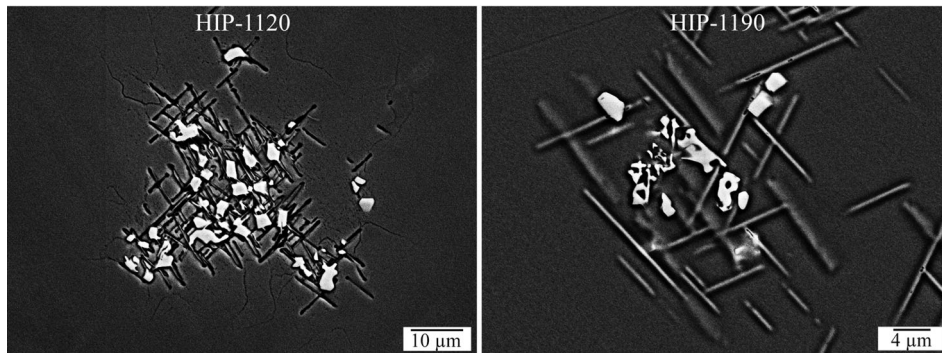


Figure 4. Backscattered images showing evolution of segregating phases in the HIP conditions.

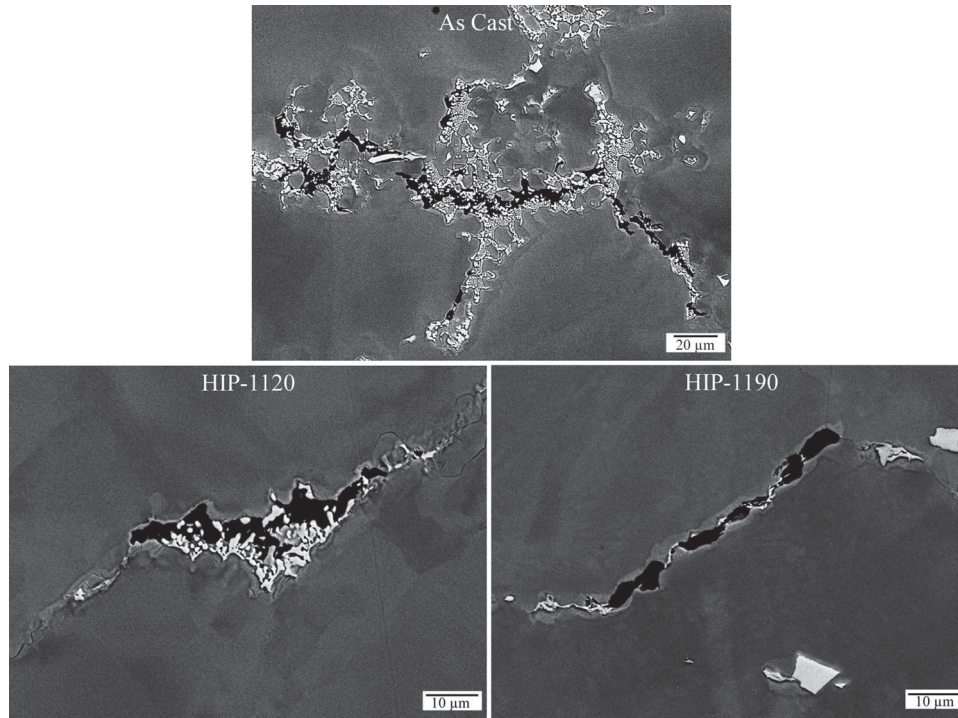


Figure 5. Backscattered SEM images showing the HAZ liquation cracking.

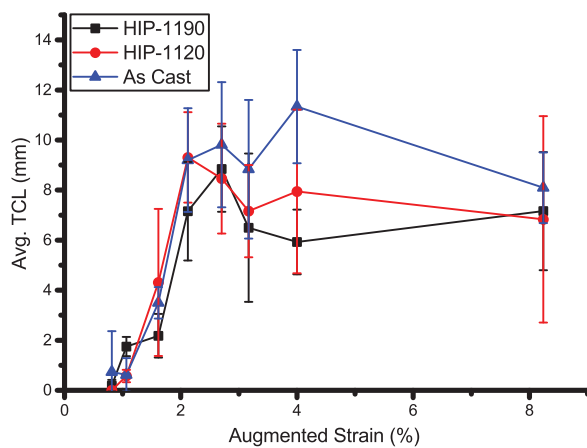


Figure 6. FZ cracking response with standard deviations for the as cast, HIP-1120 and HIP-1190 conditions.

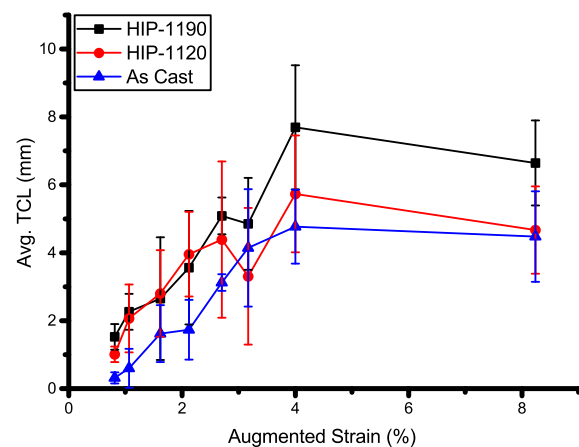


Figure 7. HAZ liquation cracking response with standard deviations for the as cast, HIP-1120 and HIP-1190 conditions.

is generally considered preferable in regards to cracking. On the other hand, the HIP conditions exhibited small cracks along the centreline grain. However, this

behaviour was not consistent among the different test plates and the authors have no explanation for these anomalies. Moreover, as it can be noticed from Table 4,

dimension/shape of weld beads varied even though welding parameters and test conditions were the same. From the literature [13], it is known about the difficulty in obtaining good penetration when welding Alloy 718 due to the poor fluidity of the molten weld metal. Small variations of minor elements in Cast Alloy 718 are also known to promote differences in weld penetration [14]. Srinivasan et al. [15] have pointed out the high variability of TCL in relation to varying weld bead geometry during longitudinal Varestraint testing.

In general, the solidification cracking data from Figure 6 reveal the typical shape of Varestraint testing curves with increasing TCL until a saturation level is reached and there is no distinction in between the different conditions. The spread of Avg. TCL at 4% augmented strain can be related to both test and also to material associated scatter. A supporting fact that the three conditions behave similarly is related to the solidification range of the alloy which is dependent on the alloy composition [16]. As it is for the current study, the base metal compositions for the three conditions are the same, so is the solidification range, as it is an intrinsic property of the material. This confirms the hypothesis that the three conditions as cast, HIP-1120 and HIP-1190 have the same solidification cracking susceptibility. Such hypothesis is supported in a study conducted by Cieslak et al. [17], where a similar response in hot cracking susceptibility for two conditions of 625 Plus, aged and annealed, was found. Cieslak et al. assumed this to be related to the melting and solidification reactions occurring in the fusion zone, consequently eliminating the thermal history.

Heat affected zone liquation cracking

The cracking response in the HAZ follows a different trend in comparison to the FZ (Figure 7). As for the FZ crack measurements, the liquation cracking response discloses a significant amount of scatter. A possible explanation for the large spread in results when testing cast material can be related to the macrosegregation

resulting from the casting process, which is not possible to eliminate completely even with the HIP treatments. Therefore, it is reasonable to expect such high variations in terms of cracking response, as the cracking behaviour of the material is dependent on local segregation condition in the cast plates especially when it comes to crack propagation properties.

The large scatter has been also reported also elsewhere in the literature [8], i.e. when conducting crack growth tests for cast Alloy 718. The same study also reflected on the high scatter for hot ductility tests. Moreover, studies regarding HAZ liquation cracking of Allvac® 718 Plus™ [18] in the wrought form, which is generally known to be more homogenised in terms of segregation, also revealed high variability from the crack measurements, with standard deviations overlapping between the different heat treatment conditions. However, despite the large scatter as can be seen in Figure 7, the as cast condition exhibits the lowest cracking susceptibility at all strain levels but 3.2% augmented strain. The HIP-1120 and HIP-1190 show similar cracking response at low strain levels, but above 2.6% the HIP-1190 has the worst behaviour as represented with the highest Avg. TCL measurements.

In the as cast condition, small and interconnected liquation cracks were seen especially in areas where Laves phase have liquated. This could be a possible explanation for the lower Avg. TCL. Generally, they followed the solidification grain boundaries present from the casting process (dashed line in Figure 8), but few small cracks were also occurring intragranularly as indicated by the arrows. With increasing HIP temperature, the amount of segregation decreased due to the dissolution of the secondary precipitates, the main effect being related to the reduction of the Laves content. This changed the cracking mechanism in the HIP conditions to grain boundary liquation mechanism as clearly visible in Figure 5. The cracks in the HIP-1120 and HIP-1190 conditions were surrounded by the presence of re-solidified products which suggests that liquid films along the grain boundaries existed prior to

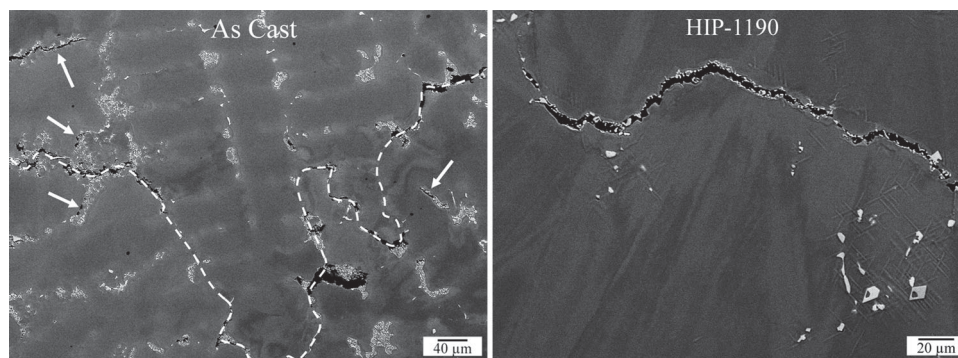


Figure 8. The picture on the left is showing HAZ liquation cracks in the as cast condition, the dashed line delineates the grain boundary and the arrows indicate locations where intergranular cracks occurred. On the right picture, liquation cracking in the HIP-1190 condition.

cracking. An explanation for this could be the enrichment of Nb from dissolution of secondary precipitates by diffusion mechanism which lowers the melting temperature. However, EDS linescans across the grain boundaries did not reveal any Nb enrichment. The reason could be that the resolution of the EDS could have been insufficient to investigate the microsegregation of Nb. Other than that, Huang et al. [19] have demonstrated by SIMS analysis the strong effect of B segregation at the grain boundaries on HAZ liquation cracking of cast Alloy 718. The higher Avg. TCL for the HIP-1190 can be related to the larger grain size for that HIP treatment. From Table 5, it can be noticed that by increasing the homogenisation temperature, not only the volume fraction of the secondary precipitates changed, also, the grain size increased. HIP-1190 exhibited the highest value of 3.3 mm, almost twice in respect to the as cast with 1.7 mm, whereas the HIP-1120 had average grain size of 2.6 mm. Figure 8 also shows a relatively long and continuous crack along the grain boundary in the HIP-1190 condition. Note the 'straightening' effect of the grain boundaries due to the increasing grain size in relation to the as cast, which had a more tortuous shape. Grain size is considered to be an important parameter when assessing the HAZ liquation cracking susceptibility. Generally, smaller grain size is believed to be beneficial in terms of resistance towards liquation cracking mainly because the larger grain boundary area allows a better strain accommodation [20]. Several studies investigating wrought and cast Alloy 718 [20–23] have agreed upon this, except of Huang et al. [24], who reported that micro cast heats with smaller grain size than the conventionally cast heats with larger grain size showed an increased cracking susceptibility, mainly due to the large amount of available liquation points.

Conclusion

Hot cracking susceptibility of three different conditions of cast Alloy 718 has been investigated by Vareststraint weldability testing method; as cast, HIP-1120 (1120°C/4h (HIP) + 1050°C/1h and furnace cooling to 650°C/1h in vacuum + 950°C/1h) and HIP-1190 (1190°C/4h (HIP) + 870°C/10h and furnace cooling to 650°C/1h in vacuum + 950°C/1h). The cracking response has been analysed in terms of susceptibility towards solidification and HAZ liquation cracking. The results indicate no difference relative to the solidification cracking susceptibility between the three conditions.

The susceptibility towards HAZ liquation cracking can be ranked as follows: HIP-1190 having the highest susceptibility, followed by HIP-1120 and the as cast having the lowest cracking susceptibility. In the current study, it was found that especially the amount of secondary precipitates and base metal grain size seem

to have a significant role in determining susceptibility towards the HAZ liquation cracking.

Acknowledgement

The authors would like to acknowledge Tommy Kan for help with Vareststraint testing.

Disclosure statement

No potential conflict of interest was reported by the authors.

Funding

The support from KME through funding from the Swedish Energy Agency and GKN Aerospace Sweden AB is highly appreciated.

ORCID

Sukhdeep Singh  <http://orcid.org/0000-0002-2572-4975>

Joel Andersson  <http://orcid.org/0000-0001-9065-0741>

References

- [1] Eiselstein HL. Age-hardenable nickel alloy. U.S. Patent No 3,046,108, 1962.
- [2] LORIA EA. The status and prospects of alloy 718. *JOM*. 1988;40(7):36–41.
- [3] Ballou OW, Coffey MW. History of Cast Inco 718. *Superalloys 1988, 1988*, 469–473.
- [4] Andersson J. Weldability of precipitation hardening superalloys—influence of microstructure [Phd Thesis]. Chalmers University of Technology; 2011
- [5] Radavich JF. The physical metallurgy of cast and wrought alloy 718. *Superalloy 718 – Metallurgy and Applications*. 1989: 229–240.
- [6] Carlson RG, Raadavich JF. Microstructural characterization of cast 718. *Int. Symp. Superalloys*; 1989. p. 79–95.
- [7] Sims CT, Stoloff NS, Hagel WC. *Superalloys II*. New York: Wiley-Interscience; 1987.
- [8] Barron ML. Crack growth-based predictive methodology for the maintenance of the structural integrity of repaired and nonrepaired aging engine stationary components. GE AIRCRAFT ENGINES CINCINNATI OH; 1999.
- [9] Snyder SM, Brown EE. Laves free cast + hip nickel base superalloy. U.S. Patent No 4,750,944; 1988.
- [10] Paulonis DF, Schirra JJ. Alloy 718 at Pratt & Whitney—Historical perspective and future challenges. *Superalloys, 2001*, 718.625,706: 13–23.
- [11] Hirko GS, Hatala RW, Mattern RA. Crack growth-based predictive methodologies for the maintenance of structural integrity of repaired and nonrepaired aging engine stationary components. PRATT AND WHITNEY EAST HARTFORD CT; 2003.
- [12] Andersson J, Jacobsson J, Lundin C. A historical perspective on Vareststraint testing and the importance of testing parameters. In: *Cracking phenomena in welds IV*. Springer International Publishing, 2016. pp. 3–23.
- [13] Gordine J. Some problems in welding inconel 718. *Weld. Res. Suppl.* 1971;50:480–484s.
- [14] Spicer RA, Baeslack III WA, Kelly TJ. Elemental effects on GTA spot weld penetration in Cast Alloy 718. *Weld. Res. Suppl.* 1990;69:285–288.

- [15] Srinivasan G, Bhaduri AK, Shankar V, et al. Evaluation of hot cracking susceptibility of some austenitic stainless steels and a nickel-base alloy. *Weld World*. 2008;52:4–17.
- [16] Pumphrey WI, Jennings PH. A consideration of the nature of brittleness at temperatures above the solidus in castings and welds in aluminium alloys. *J Inst Met*. 1948;75(4):235.
- [17] Cieslak MJ, Headley TJ, Frank RB. The welding metallurgy of custom age 625 PLUS alloy. *Weld J*. 1989;68(12):473–482.
- [18] Vishwakarma K, Chaturvedi M. A study of HAZ microfissuring in a newly developed Allvac 718 Plus superalloy. *Superalloy 2008*. TMS; 2008. pp. 241–250.
- [19] Huang X, Chaturvedi MC, Richards NL. Effect of homogenization heat treatment on the microstructure and heat-affected zone microfissuring in welded cast alloy 718. *Metall Mater Trans A*. 1996;27:785–790.
- [20] Dupont JN, Lippold JC, Kiser SD. *Welding metallurgy and weldability of nickel-base alloys*. Hoboken (NJ): John Wiley & Sons; 2009.
- [21] Thompson RG, Cassimus JJ, Mayo DE, et al. The relationship between grain size and microfissuring in alloy 718. *Weld J*. 1985;64(4):91–96.
- [22] Hong JK, Park JH, Park NK, et al. Microstructures and mechanical properties of inconel 718 welds by CO₂ laser welding. *J. Mater. Process. Technol*. 2008;201:515–520.
- [23] Woo I, Nishimoto K, Tanaka K, et al. Effect of grain size on heat affected zone cracking susceptibility study of weldability of inconel 718 cast alloy (2nd report). *Weld Intl*. 2000;14(7):514–522.
- [24] Huang X, Richards NL, Chaturvedi MC. Effect of grain size on the weldability of cast alloy 718. *Mater Manuf Processes*. 2004;19(2):285–311.